14th International Conference on Applications of Statistics and Probability in Civil Engineering, ICASP14
Dublin, Ireland, July 9-13, 2023

Seismic reliability assessment of slopes subjected to stochastic pulse-like ground motion

Guan Chen
Postdoc, Institute for Risk and Reliability, Leibniz Universität Hannover, Hannover, Germany. E-mail: guan.chen@irz.uni-hannover.de (corresponding author)

Chao Dang
PhD candidate, Institute for Risk and Reliability, Leibniz Universität Hannover, Hannover, Germany. E-mail: chao.dang@irz.uni-hannover.de

Ruohan Wang
PhD candidate, Institute for Risk and Reliability, Leibniz Universität Hannover, Hannover, Germany. E-mail: ruohan.wang@irz.uni-hannover.de

Michael Beer
Professor, Institute for Risk and Reliability, Leibniz Universität Hannover, Hannover, Germany. E-mail: beer@irz.uni-hannover.de

ABSTRACT: Near-fault pulse-like ground motions attract increasing attention in engineering because they tend to cause more severe damage to structures than ordinary ground motions. Landslides, as the most common natural hazard triggered by earthquakes, pose a critical threat to life and infrastructure safety. However, the seismic reliability assessment of slopes under near-fault pulse-like ground motions remains challenging due to the lack of records and the complexity of the dynamic response analysis. Hence, this study developed a framework for assessing the reliability of slopes under near-fault seismic excitation by integrating the pulse-like ground motion simulation method, the nonlinear dynamic analysis, and the extreme value distribution-based reliability method. A data-based empirical relationship between the design target spectrum in anti-seismic codes and seismic reliability was established for slopes, providing references for further study of seismic reliability in near-fault regions.

The near-fault pulse-like ground motions that feature long period and high amplitude in velocity have attracted increasing attention since they were reported by Housner and Hudson (1958). So far, great achievements also have been made in various aspects, such as generation principle (e.g., Somerville et al. (1997)), identification (e.g., Baker (2007); Chen et al. (2023a)), simulation (e.g., Mavroeidis and Papageorgiou (2003); Chen et al. (2022a)), and impacts on structures (e.g., Alonso-Rodríguez and Miranda (2015); Baltzopoulos et al. (2016)).

That pulse-like ground motions tend to cause severer damage on structures than ordinary ground motions is widely accepted (e.g., Phan et al. (2007); Tothong and Cornell (2008); Chen et al. (2023b)). However, most studies do not consider the randomness of pulse-like ground motions. Based on the study of Shahi and Baker (2014), about 250 pulse-like ground motions are identified in the PEER NGA-West2 database. Hence, although some studies attempt to carry out seismic reliability under pulse-like ground motions (e.g., Li et al. (2022); Pang et al. (2018); Psycharis et al. (2013)), the ef-

fects of uncertainties of near-fault pulse-like ground motions on seismic risk analysis still remain largely unexplored due to the insufficiency of pulse-like records.

This study performs the seismic reliability assessment under stochastic pulse-like ground motions by integrating the pulse-like ground motion simulation method, the finite element method, and the extreme value distribution-based reliability method. Compared with previous studies, an advantage of this study is that the target spectrum compatibility of near-fault pulse-like ground motion is considered. An unsaturated soil slope is taken as an example because landslides are one of the most common hazards in earthquakes and most soil is unsaturated naturally.

1. GROUND MOTION DATABASE

1.1. Pulse-like ground motion simulation

In accordance with the anti-seismic codes (like Eurocode8), the target spectrum-based strategy is adopted for input ground motions in this study. Since the insufficiency of pulse-like records, artificial pulse-like ground motions are simulated. Specifically, a trigonometric series-based simulation method proposed by Chen et al. (2022a) is used, which can generate target spectrum-compatible pulse-like ground motions effectively. The method is briefly introduced as follows.

A trigonometric series-based form for ground-motion velocity $\dot{u}(t)$ is proposed first, as shown in Eq. (1).

$$\dot{u}(t) = \sum_{i=1}^{n} \dot{u}_i(t) = \sum_{i=1}^{n} A(t)\cos(\omega_i t + \phi_i) \qquad (1)$$

where $\dot{u}_i(t)$ is the component of the ground-motion velocity; $A(t)$ is the amplitude modulation function, which is fixed in this study to make the simulated ground-motion velocity containing a pulse; t is the time series; ω_i is a frequency variable in the interval of $[0, \omega_s]$, in which ω_s is the half of sampling frequency of recorded ground motions; and ϕ_i is a phase variable in the interval of $[0, 2\pi]$.

Then, an iteration scheme is required to perform the summation in Eq. (1) and to make the response spectrum of simulated ground motion compatible with the target spectrum. The error ε in Eq. (2) is adopted to evaluate the compatibility between the pseudo-spectral acceleration of simulated ground motion $S_a^s(T)$ and target spectrum $S_a^t(T)$. In this study, the allowable error is set to 10%.

$$\varepsilon = \sqrt{\frac{\sum_{k=0}^{N-1}[S_a^t(T_k) - S_a^s(T_k)]^2}{\sum_{k=0}^{N-1}[S_a^t(T_k)]^2}} \qquad (2)$$

where $S_a^t(T_k)$ is the target response spectrum; $S_a^s(T_k)$ is the elastic pseudo-acceleration response spectrum of the simulated ground motion; and T_k is the corresponding period of response spectrum.

As explained above, the method requires two inputs: the amplitude modulation function and the target spectrum. The Hilbert transform of a recorded pulse-like ground motion is employed as the amplitude modulation function, and the target response spectrum for Spectra Type 1 and Ground Type C in Eurocode8 is used, as shown in Figure 1. Further details can be found in Chen et al. (2022a).

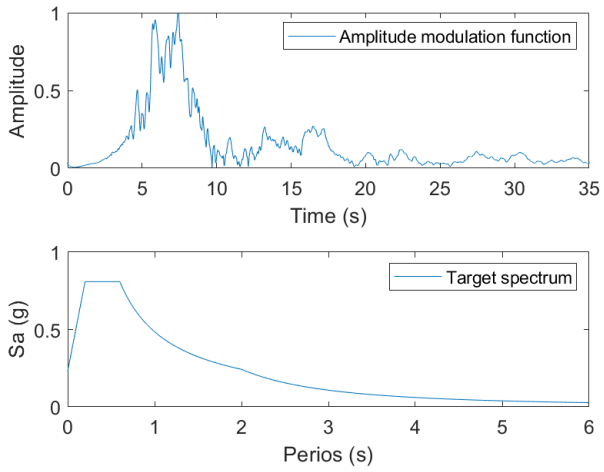

Figure 1: Amplitude modulation function and target spectrum used in the method for simulating pulse-like ground motions.

An example of simulated pulse-like ground motion is shown in Figure 2, in which the velocity, the acceleration, and the spectral velocity and acceleration of the ground motion are provided. It is shown that a pulse exists in velocity, and the response spectrum of simulated ground motion is compatible with the target spectrum.

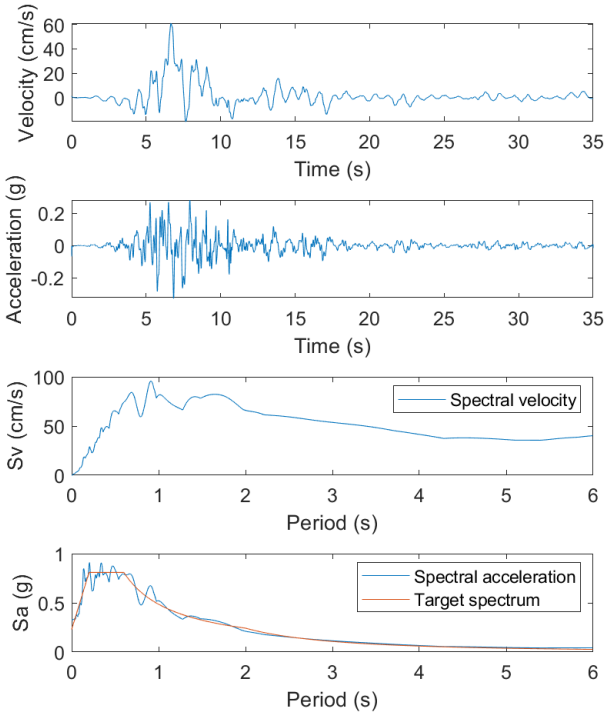

Figure 2: Example of simulated pulse-like ground motion.

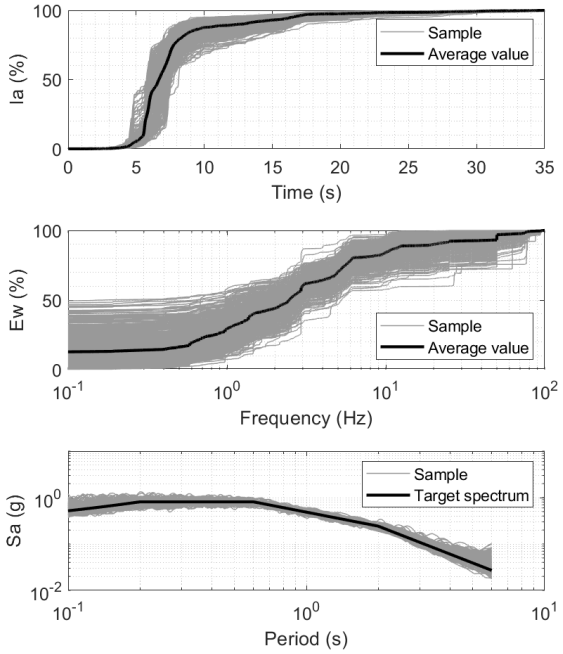

Figure 3: Arias intensity (I_a), wavelet-based normalized cumulative energy (E_w), and spectral acceleration (S_a) of one thousand simulated pulse-like ground motions.

1.2. Ground motion intensity measures

One thousand pulse-like ground motions that are compatible with the same target spectrum are generated. To describe the time- and frequency-domain characteristics of simulated ground motions, three common intensity measures, including the Arias intensity, response spectrum, and frequency-domain energy distribution, are provided, as shown in Figure 3. The wavelet packet transform is applied to perform the time-frequency analysis due to the advantages of high resolution on the low-frequency region (see Chen et al. (2019)).

Figure 3 shows that (i) the average significant duration (D_{5-75}) of simulated ground motions is 2.83 s (4.92 s - 7.75 s). (ii) About 30 % of energy distributes in the very low-frequency regions (0 Hz - 1 Hz), which agrees with the previous study of Chen et al. (2022b, 2023b). This feature potentially makes pulse-like ground motions cause severer damage to structures with high fundamental periods. (iii) The spectral accelerations of simulated ground motions are compatible with the target spectrum effectively.

2. SEISMIC RESPONSE OF SLOPE

2.1. Finite element model

The seismic response analyses of an unsaturated clayey soil slope are performed under simulated pulse-like ground motions, where the dynamic unified hardening constitutive model (see Luo et al. (2020)) is utilized to characterize the unsaturated clayey soil properties. Technically, a three-dimensional finite element analysis is conducted by combining a coupling-based hydro-mechanical analysis based on ABAQUS software with user subroutines written in FORTRAN. The geometric dimensions and finite element mesh of the slope model are depicted in Figure 4. The model consists of 9840 elements which are all 8-node elements with reduced integration (C3D8R). The boundary conditions of the model are as follows: the upper part is a free surface; the surrounding is an absorbing surface; the bottom is rigid, and the displacement in the y-axis directions is fixed. The ground motion is inputted from the bottom in the x-axis direction. Material properties of clay soil in Luo et al. (2020) are used, as listed in Table 1. The mass-proportional coefficient and stiffness-

proportional coefficient of Rayleigh damping for the slope model are assumed to be 2.4354 and 0.0008. The fundamental period of the slope is 1.32 s.

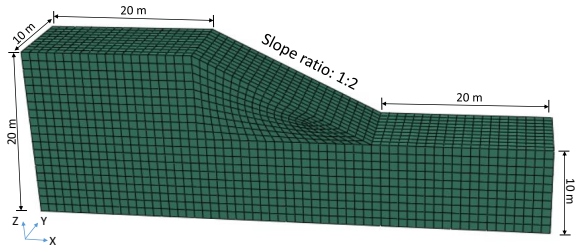

Figure 4: Finite element model.

2.2. *Seismic slope displacement*

To characterize the effects of ground motion uncertainty on seismic response, one thousand times Monte Carlo simulations are performed. An example of the seismic slope displacement is shown in Figure 5. Further analyses of the Monte Carlo simulations are carried out in the next Section.

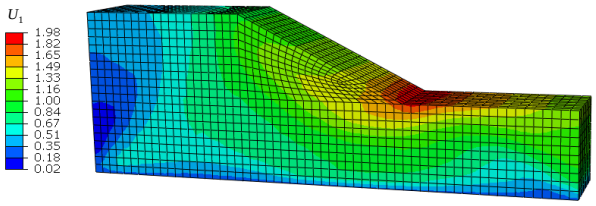

(a) Totoal displacement

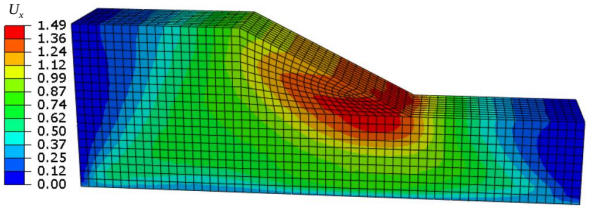

(b) x-axis direction displacement

Figure 5: Seismic displacement response of slope.

3. SEISMIC RELIABILITY ASSESSMENT

Under the above settings, it is possible to assess the seismic reliability of the slope under stochastic pulse-like ground motions with the help of the theory and methods of dynamic reliability analysis. To do so, we turn the reliability problem into a first-passage one and define the first-passage probability of the slope as:

$$P_f = \Pr\{|X(t)| > \delta, \exists t \in [0,T]\}, \tag{3}$$

where $X(t)$ represents a stochastic response process of the slope, which is of interest for seismic reliability analysis; δ is a prescribed threshold. Eq. (3) can be equivalent to:

$$P_f = \Pr\{Y > \delta\}, \tag{4}$$

where $Y = \max_{t\in[0,T]} |X(t)|$. It is obvious that once the probability distribution of Y (referred to as extreme value distribution) is obtained, P_f can be determined accordingly.

In this study, the moment-generating function based mixture distribution (MGF-MD) method (Dang et al. (2021)) is adopted to approximate the extreme value distribution. First, we assume that Y follows a mixture distribution, called mixture of two generalized inverse Gaussian distributions (MTGIGD). The probability density function (PDF) of MTGIGD reads:

$$\begin{aligned} f(y) =& \varpi\, f_0(y;\alpha^{(1)},\beta^{(1)},\lambda^{(1)}) \\ &+ (1-\varpi)\, f_0(y;\alpha^{(2)},\beta^{(2)},\lambda^{(2)}), \end{aligned} \tag{5}$$

where $0 < \varpi < 1$, $\alpha^{(1)} > 0$, $\beta^{(1)} > 0$, $\lambda^{(1)} \in \mathbb{R}$, $\alpha^{(2)} > 0$, $\beta^{(2)} > 0$ and $\lambda^{(2)} \in \mathbb{R}$ are seven free parameters; $f_0(y;\alpha,\beta,\lambda)$ represnts the PDF of a generalized inverse Gaussian distribution (GIGD), which is defined as:

$$f_0(y;\alpha,\beta,\lambda) = \frac{(\alpha/\beta)^{\lambda/2}}{2K_\lambda(1)\left(\sqrt{\alpha\beta}\right)} y^{(\lambda-1)} e^{-(\alpha y+\beta/y)/2}, \tag{6}$$

where K_λ is a modified Bessel function of the second kind with order λ. The MGF of MTGIGD is given by:

$$\begin{aligned} M(\tau) =& \varpi\, M_0(\tau;\alpha^{(1)},\beta^{(1)},\lambda^{(1)}) \\ &+ (1-\varpi)\, M_0(\tau;\alpha^{(2)},\beta^{(2)},\lambda^{(2)}), \end{aligned} \tag{7}$$

where $M_0(\tau;\alpha,\beta,\lambda)$ denotes the MGF of a GIGD such that:

$$M_0(\tau;\alpha,\beta,\lambda) = \left(\frac{\alpha}{\alpha-2\tau}\right)^{\frac{\lambda}{2}} \frac{K_\lambda\left(\sqrt{\beta(\alpha-2\tau)}\right)}{K_\lambda\left(\sqrt{\alpha\beta}\right)}. \tag{8}$$

Table 1: Mechanical parameters of soil materials

Parameters	λ (-)	κ (-)	M (-)	ν (-)	N (-)	$\varphi(^\circ)$	a (kPa)	p^c (kPa)	$\psi(^\circ)$	κ_s (-)	ρ (g/cm^3)
Value	0.105	0.020	1.0	0.3	1.316	10	200	50	0	0.01	1.92

Then, those seven parameters can be determined by matching the MGF of MTGIGD with that of Y at seven discrete values. Here, the MGF of Y can be estimated by its 1000 samples from MCS such that:

$$\hat{M}(\tau) = \frac{1}{1000} \sum_{i=1}^{1000} \exp(\tau y^{(i)}) \tag{9}$$

where $y^{(i)}$ denotes the i-th sample of Y. For more details, one can refer to Dang et al. (2021).

We take the displacements of the slope as an example to demonstrate the MGF-MD method. The PDF and 1-CDF (cumulative distribution function) of the maximum absolute total displacement are compared in Figure 6. It is shown that the MGF-MD method is able to well approximate the maximum absolute total displacement. From the 1-CDF plot, one can obtain the first-passage probability given a threshold δ. For example, the failure probability is predicted to be 3.27×10^{-4} if $\delta = 5$ m. Besides, the results of the maximum absolute displacement along x-axis are also given in Figure 7.

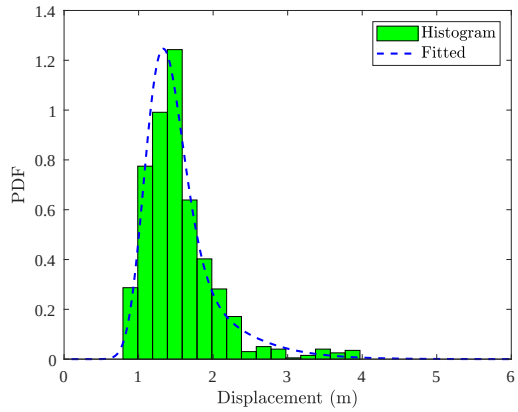

(a) PDF

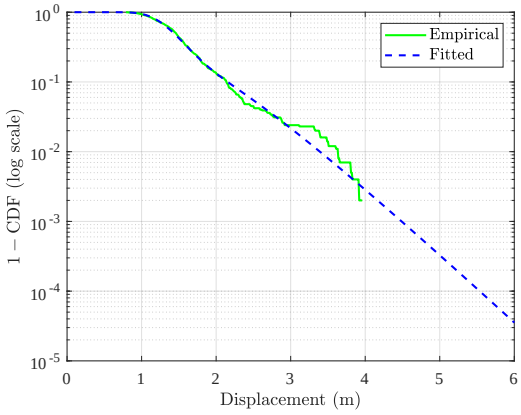

(b) 1-CDF

Figure 6: PDF and 1-CDF of the maximum absolute total displacement.

4. CONCLUSIONS

A framework is formulated to perform seismic reliability analysis in near-fault regions by integrating a stochastic pulse-like ground motion simulation method, a finite element method, and an extreme value distribution-based reliability method. An application on an unsaturated soil slope is performed to verify its effectiveness and efficiency. Results show that the proposed method offers a promising approach to connect the target spectrum and the seismic failure probability in near-fault regions.

However, this study may underestimate the uncertainties of pulse-like ground motions compared to natural records since the amplitude modulation function and the target spectrum are fixed in the ground motion simulation method. Besides, since the uncertainties of ground motion dominate the seismic response, the uncertainties of soil properties in the slope are ignored.

5. ACKNOWLEDGMENTS

This research is supported by the International Joint Research Platform Seed Fund Program of Wuhan University (Grant No. WHUZZJJ202207). Chao Dang and Ruohan Wang have received the financial support from China Scholarship Council (CSC). Guan Chen would like to thank the financial support of Sino-German (CSC-DAAD) Postdoc Scholarship Program.

6. REFERENCES

Alonso-Rodríguez, A. and Miranda, E. (2015). "Assessment of building behavior under near-fault pulse-like

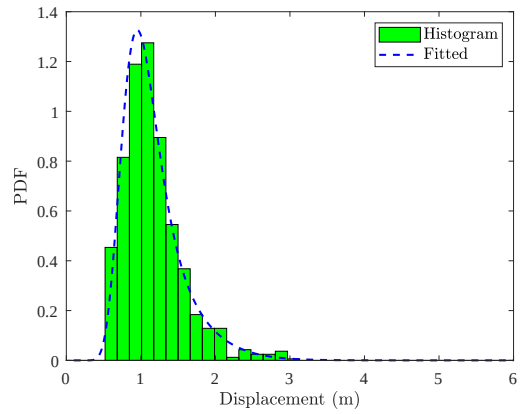

(a) PDF

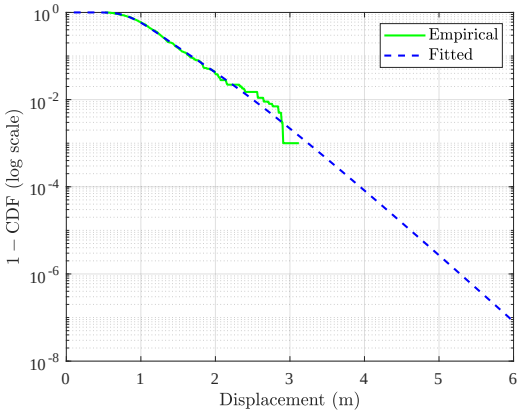

(b) 1-CDF

Figure 7: PDF and 1-CDF of the maximum absolute displacement along x-axis.

ground motions through simplified models." *Soil Dynamics and Earthquake Engineering*, 79, 47–58.

Baker, J. W. (2007). "Quantitative classification of near-fault ground motions using wavelet analysis." *Bulletin of the Seismological Society of America*, 97(5), 1486–1501.

Baltzopoulos, G., Vamvatsikos, D., and Iervolino, I. (2016). "Analytical modelling of near-source pulse-like seismic demand for multi-linear backbone oscillators." *Earthquake Engineering & Structural Dynamics*, 45(11), 1797–1815.

Chen, G., Beer, M., and Liu, Y. (2022a). "Modeling response spectrum compatible pulse-like ground motion." *Mechanical Systems and Signal Processing*, 177, 109177.

Chen, G., Li, Q.-Y., Li, D.-Q., Wu, Z.-Y., and Liu, Y. (2019). "Main frequency band of blast vibration signal based on wavelet packet transform." *Applied Mathematical Modelling*, 74, 569–585.

Chen, G., Liu, Y., and Beer, M. (2022b). "Frequency comparison of the pulse-like and non-pulse ground motions." *Proceedings of 8th International Symposium on Reliability Engineering and Risk Management (ISRERM2022)*, 277–281.

Chen, G., Liu, Y., and Beer, M. (2023a). "Identification of near-fault multi-pulse ground motion." *Applied Mathematical Modelling*, 117, 609–624.

Chen, G., Yang, J., Liu, Y., Kitahara, T., and Beer, M. (2023b). "An energy-frequency parameter for earthquake ground motion intensity measure." *Earthquake Engineering & Structural Dynamics*, 52(2), 271–284.

Dang, C., Wei, P., and Beer, M. (2021). "An approach to evaluation of EVD and small failure probabilities of uncertain nonlinear structures under stochastic seismic excitations." *Mechanical Systems and Signal Processing*, 152, 107468.

Housner, G. W. and Hudson, D. E. (1958). "The Port Hueneme earthquake of March 18, 1957." *Bulletin of the Seismological Society of America*, 48(2), 163–168.

Li, L., Fang, M., Chen, G., and Yang, D. (2022). "Reliability-based stochastic optimal control of frame building under near-fault ground motions." *Mechanical Systems and Signal Processing*, 163, 108098.

Luo, T., Chen, D., Yao, Y.-P., and Zhou, A.-N. (2020). "An advanced uh model for unsaturated soils." *Acta Geotechnica*, 15(1), 145–164.

Mavroeidis, G. P. and Papageorgiou, A. S. (2003). "A mathematical representation of near-fault ground motions." *Bulletin of the Seismological Society of America*, 93(3), 1099–1131.

Pang, R., Xu, B., Kong, X., Zhou, Y., and Zou, D. (2018). "Seismic performance evaluation of high cfrd slopes subjected to near-fault ground motions based on generalized probability density evolution method." *Engineering Geology*, 246, 391–401.

Phan, V., Saiidi, M. S., Anderson, J., and Ghasemi, H. (2007). "Near-fault ground motion effects on reinforced concrete bridge columns." *Journal of Structural Engineering*, 133(7), 982–989.

Psycharis, I. N., Fragiadakis, M., and Stefanou, I. (2013). "Seismic reliability assessment of classical columns subjected to near-fault ground motions." *Earthquake Engineering & Structural Dynamics*, 42(14), 2061–2079.

Shahi, S. K. and Baker, J. W. (2014). "An efficient algorithm to identify strong-velocity pulses in multicomponent ground motions." *Bulletin of the Seismological Society of America*, 104(5), 2456–2466.

Somerville, P. G., Smith, N. F., Graves, R. W., and Abrahamson, N. A. (1997). "Modification of empirical strong ground motion attenuation relations to include the amplitude and duration effects of rupture directivity." *Seismological Research Letters*, 68(1), 199–222.

Tothong, P. and Cornell, C. A. (2008). "Structural performance assessment under near-source pulse-like ground motions using advanced ground motion intensity measures." *Earthquake Engineering & Structural Dynamics*, 37(7), 1013–1037.